Received: 10 April 2017 | Revised: 25 August 2017 | Accepted: 28 August 2017

DOI: 10.1002/chir.22770

REGULAR ARTICLE

WILEY

Absolute configuration assignment of (+)-fluralaner using vibrational circular dichroism

John Kong[2] | Leo A. Joyce[3] | Jinchu Liu[3] | Tiffany M. Jarrell[2] | J. Chris Culberson[1] | Edward C. Sherer[1]

[1] Modeling & Informatics, MRL, Rahway, New Jersey

[2] Animal Health, Intervet, Inc., Rahway, New Jersey

[3] Process Research & Development, MRL, Rahway, New Jersey

Correspondence
Edward Sherer, Modeling & Informatics, MRL, Rahway, NJ 07065, USA.
Email: edward_sherer@merck.com

Abstract

The absolute configurations of the separated enantiomers of fluralaner, a racemic animal health product used to prevent fleas and ticks, have been assigned using vibrational circular dichroism (VCD). The crystallographic structure of the active enantiomer (+)-fluralaner has previously been shown to have the (*S*) configuration using small molecule crystallography. We sought a faster analytical method to determine the absolute configuration of the separated enantiomers. When comparing the measured IR (infrared) and VCD spectra, it is apparent that the amide carbonyl groups appear in the IR but are nearly absent in the VCD. Computational work to calculate the VCD and IR using in vacuo models, implicit solvation, and explicitly solvated complexes has implicated conformational averaging of the carbonyl VCD intensities.

KEYWORDS

absolute configuration, Bravecto, DFT, fluralaner, VCD, vibrational circular dichroism

1 | INTRODUCTION

Accurate assignment of the absolute configuration of a chiral drug is an extremely important task in pharmaceutical research and development. Approximately 50% of marketed drugs are chiral with roughly half of those drugs containing a mixture of enantiomers.[1] When a chiral drug is introduced in vivo, the enantiomers may display dramatically different biological activities. While one enantiomer may be active in eliciting the desired medicinal effect, the other enantiomer may be either inactive or contribute to undesired side effects.[1] The following are a few pharmaceutical examples of enantiomers showing different bioactivities: *R*-thalidomide has been marketed as a sedative while *S*-thalidomide has been shown to cause severe birth defects; *R*-naproxen is used for arthritic pain while *S*-naproxen is teratogenic; and D-ethambutol is an antituberculosis drug while L-ethambutol has been found to cause blindness.[2] For this reason, enantiomers must be studied as individual entities or carefully controlled analytically unless proven differently.

Fluralaner, an isoxazoline-containing compound shown in Scheme 1, is used to repel ticks for dogs and fleas for cats. It is an insecticide/parasiticide that was first synthesized by Nissan Chemical Industries, Ltd, targeting γ-aminobutyric acid (GABA) receptors and chloride-gated glutamate channels.[3] Fluralaner is dosed as a racemic mixture of *R*- and *S*-enantiomers. Previously, single crystal X-ray crystallography (SCXRD) has been used to assign the absolute configuration of fluralaner.[3] Studies of fluralaner have shown that the *R*-enantiomer is inactive while the *S*-enantiomer is biologically active.[3]

While the absolute configuration of the active enantiomer, or (+)-fluralaner, was assigned using SCXRD, growing a single crystal can be time-consuming and hence additional methods were explored to assign absolute configuration without the need for crystallization. The current study uses vibrational circular dichroism (VCD) as an

 © 2017 Wiley Periodicals, Inc.

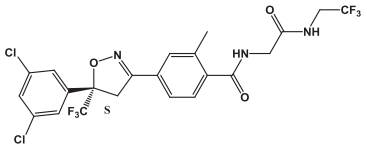

SCHEME 1 Chemical structure of fluralaner

alternative approach to identify the *R*- and *S*-enantiomers of fluralaner. The VCD chiroptical technique of combining experimental VCD spectra with density functional theory (DFT) calculated spectra has proven to be an accurate way for determining the absolute configuration of chiral molecules.[4-12] At MRL (Merck Research Laboratories), the absolute configurations of more than 350 diverse compounds have been assigned, most of which remain proprietary, but some of which have supported publications.[5,13-18] The diversity in chemical structure has led to an accumulation of experience in dealing with a vast array of chemistry complexities and functionalities when applying VCD. Commonly, it is possible to identify all functional groups of a given molecule in the VCD spectrum. During assignment of the configuration of fluralaner, a comparison of measured and computed IR and VCD spectra revealed a distinct lack of peaks (ie, nearly zero intensity) corresponding to carbonyl stretches in the VCD spectrum. A series of computational studies which explain these observations are presented.

2 | MATERIALS AND METHODS

In order to obtain pure enantiomeric samples of fluralaner, chiral prep supercritical fluid chromatography (SFC) was performed on the racemic mixture. Separation was achieved using a Chiralpak IA column (30 × 250 mm I.D., with 5 μm) with an isocratic mobile phase: CO2 /MeOH (60/40). In order to separate sufficient quantity for VCD analysis, a series of 30 stacked injections was used with the following parameters: concentration of 50 mg/mL, injection vol of 0.5 mL, flow rate of 70 mL/min, back pressure of 100 bar, temperature at 35°C, and detection at 254 nm. The final product enantiomers after separation had ee values for A and B measured at >99.9% and 97.9%, respectively.

Samples A (optical rotation: +56.2 at 589 nm, 25°C) and B of fluralaner were dissolved in $CDCl_3$ (50 mg/mL for each sample). All experiments were performed using a 0.10-mm path length cell with BaF_2 windows. The IR and VCD spectra were recorded using a ChiralIR VCD spectrometer equipped with the Dual PEM accessory (BioTools, Jupiter, Florida), with 4 cm^{-1} resolution. A dry N_2 purge was used to eliminate water from the instrument. Data were collected in blocks, where the instrument recorded approximately 3000 scans over the course of 1 hour and averaged those scans into one block. Each of the runs involved averaging 5 blocks for each sample, as well as the solvent. The solvent background average was then subtracted from the sample average. Collection times for samples and solvent were approximately 5 hours each. The VCD spectra for each enantiomer were further corrected using the respective enantiomer.

The general approach for VCD assignment at MRL, including the detailed computational workflow, has been published elsewhere.[5] Based on the generation of a diverse set of molecular mechanics conformations, we cluster conformations to a target representative set. These conformers are then sent for refinement using density functional theory. The vast majority of assignments can be accurately made using only in vacuo calculations; however, when mismatches in the spectra are observed, we pursue higher level or implicitly (and explicitly) solvated calculations. Conformers of each test structure were geometry optimized at the B3LYP/6-31G** level, and stationary points were confirmed by performing frequency calculations.[19-27] Calculated IR spectra saw improvement in quantitative peak positioning when the compounds were further minimized within the Solvation Model based on Density (SMD) implicit solvent model of chloroform.[28] All calculations were performed using Gaussian 09.[29] Output from the frequency calculation is used to extract the IR and VCD spectra.[30] Frequencies were initially scaled by a value of 0.98 but are further scaled during comparison of experimental and computational spectra.

Output conformers were ranked according to DFT energy, and a clustering was performed to remove duplicates. Two Boltzmann distributions were calculated based on either the electronic energy (E) or the free energy (G). The method for comparing spectra is based on a published algorithm for calculating similarity between the experimental and calculated IR or VCD spectra.[31] The following modifications were introduced to the algorithm: scale the spectra (0 to 1 for IR, −1 to 1 for VCD) before comparing; isolation of each peak for movement as opposed to shifting groups of peaks; isolation of peaks independently for IR and VCD spectra; peaks shifted by a default maximum shift of 25 cm^{-1}; baseline correction of the experimental spectrum when needed. When adjacent peaks are shifted relative to each other, a gap in the spectrum is introduced. The algorithm fits the disjoint ends of adjacent peaks to a parabola for a smooth transition by employing a three-point parabolic fit using the last 2 data points of the left most peak and the first point of the next peak. The method uses an overlap integral to estimate the fit which translates to a range of possible fit values of −1.0 to 1.0 for the VCD curve and 0.0 to 1.0 for the IR. The enantiomeric similarity index, or ESI, is the difference in fit of one enantiomer minus the other.

Any choice of computational method when performing VCD calculations may lead to artifacts in the overlay of spectra owing to whether calculated modes are robust or nonrobust.[32,33] In the current study, all peaks noted in the experimental spectrum were present in the computed spectrum so this methodology was not applied in this study. As will be discussed, carbonyl peaks were present in the calculated spectrum only in the absence of a proper Boltzmann population of conformations.

3 | RESULTS AND DISCUSSION

3.1 | Experimental spectra

Experimental determination of the VCD and IR spectra for fluralaner was initially considered rather straightforward. Fluralaner is sufficiently soluble in chloroform for the spectra to be clean, and upon solvent subtraction, baseline correction, and enantiomer correction, the spectra shown in Figure 1 were obtained. From the IR panel, it is clear that all fluralaner functional groups are present. However, despite sharp peaks in the region from 1000 to 1500 cm^{-1} in the measured VCD spectrum, the region 1600 to 1800 cm^{-1} where carbonyl signals are expected is conspicuously flat. Of the assignments of absolute configuration which have been performed at MRL, this represents the first example of a compound containing amide bonds which does not display carbonyl peaks in the measured VCD spectrum. To better understand this observation, additional computational experiments were explored.

3.2 | Conformational search

An initial conformational search of fluralaner was performed in vacuo using B3LYP/6-31G** and which identified four dominant conformations that are depicted in Figure 2. The structure modeled was arbitrarily chosen as the (*R*)-configuration, since the spectra calculated for enantiomers by definition will be equal and opposite. Percentage contribution to the in vacuo Boltzmann distributions are included in Figure 2 and total 78% for the electronic energy weighted distribution of the top four conformers, but these same conformers contribute only 24% to the free energy distribution. This is indicative of a conformationally diverse landscape. Free energy ranking of the conformers provides 22 conformers which contribute >1% to the distribution with nine conformers contributing >5% to a total of 54%. Coordinates for dominant minima are provided in Figure S1 Supporting Information.

The major unifying feature of the dominant conformers, as ranked by electronic energy, is the presence of an intramolecular hydrogen bond (see NH---O═C in conformer 1) between the two amide functional groups (conformers 1-4). The main structural difference between conformer pairs 1, 2 and 3, 4 is a dihedral rotation of 180° about the dihydroisoxazole-phenyl bond. Though the intramolecular hydrogen bond dominates the enthalpic energy, there is an entropic penalty to forming this bond. This entropic penalty is mostly due to the need to fold the amide tail back upon itself. Further minimization of the in vacuo conformers in implicit chloroform provides similar energetic distributions with the four dominant electronic energy minima equivalent to those shown in Figure 1, however contributing only 63% to the Boltzmann weighted spectrum compared to 78% for the calculations performed in vacuo.

3.3 | In vacuo matching

Separated enantiomeric Samples A and B were individually compared to the in vacuo Boltzmann weighted calculated IR and VCD spectra of the (*R*)-configuration. Experience indicates that an IR match of 0.7 to 0.9 represents a strong confirmation of the 2D functionality of the molecule, and a VCD match in the range of 0.2 to 0.8 represents a good VCD match. A larger ESI provides more confidence in the assignment of configuration. The initial conformer search performed is not described in detail

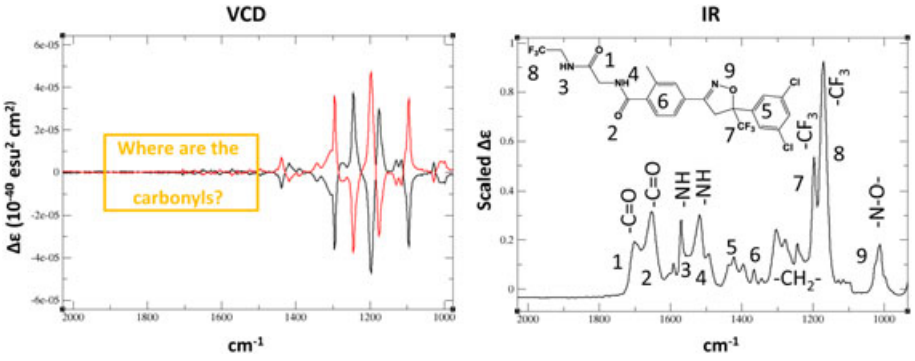

FIGURE 1 Measured IR and enantiomer-corrected VCD spectra for fluralaner (Sample A = black, Sample B = red). Curiously absent are any VCD signals corresponding to the two carbonyl functional groups clearly evident in the IR

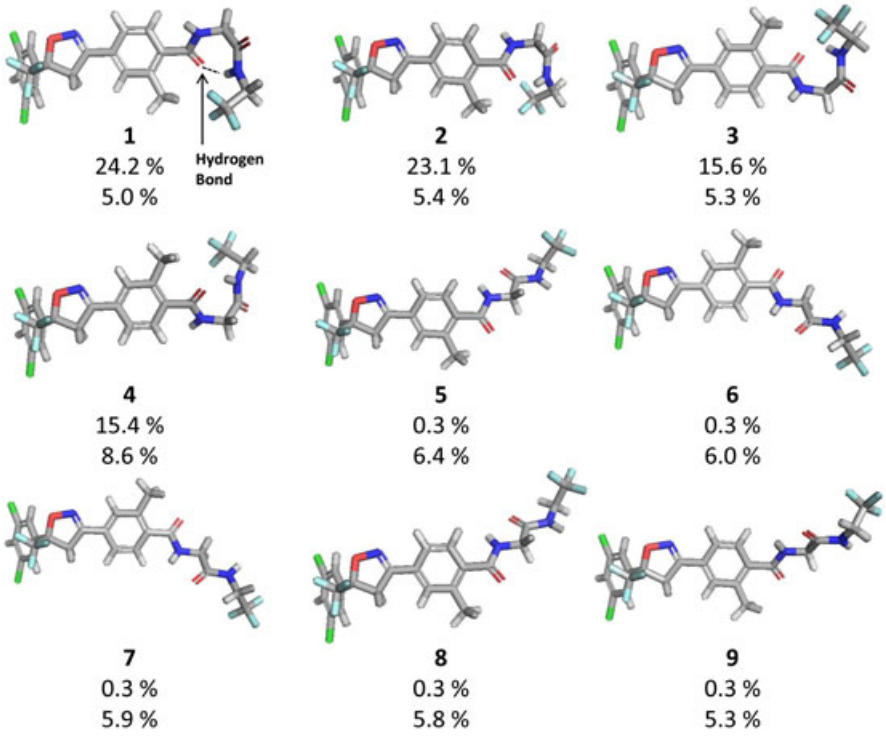

FIGURE 2 Conformations contributing to the Boltzmann conformational distribution. Electronic energy contribution (top) and free energy contribution (bottom) percentages are shown. Atom coloring: grey = carbon; red = oxygen; blue = nitrogen; green = chlorine; cyan = fluorine; white = hydrogen

here but led to an undersampled conformer distribution. Initial matching from this early conformational search of the target compound indicated significant confidence in the assignment; however, peaks in the calculated VCD spectrum corresponding to carbonyl stretches were not present in the experimental VCD spectrum. This lack of agreement between calculated and experimental spectra led to additional calculations.

3.4 | Conformational dependence

Figure 3 provides an overlay of the calculated VCD spectra for the four most dominant electronic energy conformations. These spectra show a high degree of variability in the peak intensities, and more importantly in the peak directionality. Some peaks at the low end of the spectrum are consistent across conformers and Boltzmann weighting will not average them out. Peaks in the carbonyl region may cancel each other out during Boltzmann averaging but only if they are equally sampled. Poor conformational sampling can easily lead to unbalanced populations of the dominant conformer subsets leading to residual peak signals in the 1600 to 1800 cm^{-1} range. Poor sampling was apparent in the first conformational sampling of fluralaner as the molecule exhibited a more conformationally diverse landscape than expected. This is evidenced by the difficulty of locating conformers 1 or 4 in the original search. Analysis of the distribution of conformers contributing less to the Boltzmann weighted spectrum indicated major drivers for conformational subsets were rotamers of both the phenyl and amide dihedrals. To resolve the expected undersampling, the conformer search was extended to generate the Boltzmann weighted spectra shown in Figure 4. For extended sampling, the target number of diverse conformers was increased from 50 to 150 conformations.

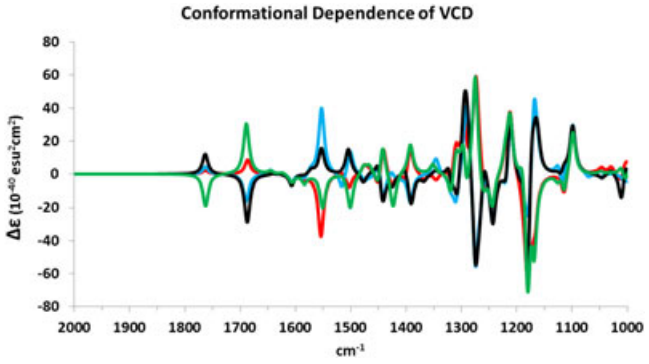

FIGURE 3 Conformational dependence on calculated in vacuo VCD spectra (conformers 1-4 = black, red, green, and blue, respectively)

With a more experimentally relevant conformer set, it was apparent that the lack of carbonyl signals in the measured VCD was due to conformational averaging of the signal. This was only effectively matched computationally with proper conformational sampling. Anytime the distribution was unbalanced, residual peak signals were noted in the computed VCD. Compounds containing carbonyls are known to occasionally be problematic owing to the robustness of modes. Nicu et al have shown that absolute

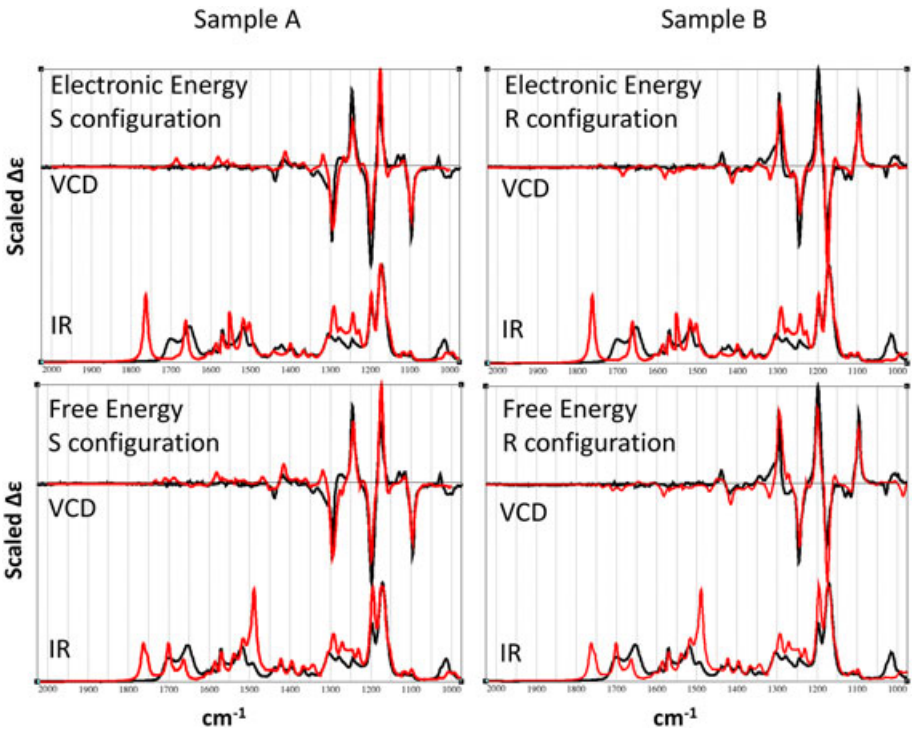

FIGURE 4 Overlay of in vacuo IR and VCD spectra for Samples A and B (calculated spectra in red, experimental spectra in black)

configuration assignment of pulegone is dependent on the application of robust mode filtering due to the conformation of the carbonyl.[32,33] In the case of fluralaner, the lack of peak intensity in the experimental spectrum is explained through cancellation of peaks via conformational averaging.

From Figure 4, the absolute configuration for Sample A ((+)-fluralaner) and Sample B ((−)-fluralaner) can be assigned *S* and *R*, respectively. Sample A is the active (+)-enantiomer, and thus the VCD analysis confirms earlier crystallographic assignment of (*S*) as the active species.[3] Table 1 provides match statistics of the curve overlays showing that the active enantiomer *S* for Sample A has a final IR and VCD match of 0.78 and 0.74 with a very significant ESI of 0.79. For the in vacuo IR, the curve fit is accurate across much of the range. However, the carbonyl stretch at approximately 1780 cm^{-1} shows evidence of a solvent shift. Since the default shifting algorithm was limited to shifting individual peaks 25 cm^{-1}, it fails to shift that peak in the calculated spectrum to overlay completely with the corresponding observed peak. The algorithm can shift peaks by 0 to 100 cm^{-1}, but we find values >25 lead to problems with peaks crossing over each other. The lower panels in Figure 4 provide the free energy weighted overlays which have similar match statistics. The main difference in the electronic energy and free energy calculated IR spectra is the presence of a dominant IR stretch approximately 1500 cm^{-1}, corresponding to an NH vibrational mode only present in the extended (nonintramolecular hydrogen bonded) conformers 5 to 9. This difference is shown in Figure 5 by observing the overlay of two computed IR spectra for conformers 1 and 5. Since the free energy IR is dominated by this NH stretch, which is not represented as dominant in the experimental IR, the electronic energy distribution dominated by four conformers provides a better representation of the experimentally relevant conformers.

While the statistics or overlays are not included, the effect of assigning the absolute configuration of Samples A and B using individual conformers from Figure 2 was investigated. Since the low range of the VCD spectrum dominates the match, even when there are residual peaks in the carbonyl range, the assignments remain *S* for Sample A and *R* for Sample B.

3.5 | Implicit chloroform

While the statistical significance of the enantiomer assignment was very high with the in vacuo modeling of fluralaner, the observation of significant intramolecular hydrogen bonding of the amides led us to consider the possibility that, in chloroform, this interaction might be interrupted through first shell solvation. Additionally, even though the spectra matching algorithm shifts peaks by up to 25 cm^{-1}, the largest observed variation in experimental IR peaks compared to the computed spectrum was the carbonyl stretches. From Figure 4, the position of the terminal carbonyl is at approximately 1760 cm^{-1}

TABLE 1 Matching statistics of the IR and VCD spectra (1000-2000 cm^{-1})[a]

	Initial IR	Final IR	Final VCD *R*	Final VCD *S*	ESI
In vacuo					
Electronic energy					
Sample A	0.63	0.78	−0.05	0.74	0.79
Sample B	0.63	0.77	0.74	−0.05	0.79
Free energy					
Sample A	0.61	0.75	−0.01	0.78	0.79
Sample B	0.61	0.75	0.78	−0.01	0.79
Electronic energy (Supporting Information, 1000-1500 cm^{-1})					
Sample A	0.68	0.89	−0.05	0.75	0.80
Implicit $CHCl_3$					
Electronic energy					
Sample A	0.71	0.73	0.26	0.44	0.18
Sample B	0.71	0.73	0.44	0.26	0.18
In vacuo with 2 explicit $CHCl_3$					
Electronic energy					
Sample A	0.61	0.71	−0.33	0.68	1.01
Sample B	0.61	0.71	0.68	−0.33	1.01
Free energy					
Sample A	0.57	0.69	−0.10	0.67	0.77
Sample B	0.57	0.68	0.67	−0.10	0.77
Implicit $CHCl_3$ with 2 explicit $CHCl_3$					
Electronic energy					
Sample A	0.70	0.70	0.21	0.37	0.16
Sample B	0.70	0.70	0.37	0.21	0.16
In vacuo fragment (without bis-amide tail)					
Electronic energy					
Sample A	0.47	0.61	−0.07	0.81	0.88

[a]Description of the curve matching and derivation of ESI is provided in Materials and Methods

while the central carbonyl is at approximately 1690 cm^{-1}. When implicit solvation is included the carbonyl stretches shift by 20 cm^{-1} in the calculated spectra to 1740 and 1670 cm^{-1}. The experimental peaks are at 1700 and 1650 cm^{-1}, which requires a shift from the in vacuo or implicit IR peaks of 60 and 40 cm^{-1}. This is too great a shift for the algorithm, although these peaks correspond to each other qualitatively. While the algorithmically allowed shift could be set to have larger maximum shifts for accommodation of solvent shifting, this causes artifactual problems in the alignment of the rest of the spectrum since peaks tend to cross over one another.

Figure 6 provides the overlays of the computed IR and VCD spectra in implicit chloroform. This approach maintains the assignment of enantiomers that had been made using in vacuo methodology. Statistics of the match in Table 1 indicate the ESI has decreased significantly from 0.80 to 0.18. Absolute configuration of Sample A would still be assigned as (*S*) and not (*R*) due to the better fit. However, owing to initial solvent shifting of selected regions of the IR and VCD spectra, the algorithm is able to shift the improper computed enantiomeric spectrum to overlay with the measured spectrum to a much greater extent than with the in vacuo spectra. The overlays of the incorrect enantiomers have not been included but they are much worse than the overlays shown in Figure 6 as they show evidence of improper peak shifting done to force a match. For this reason, even though modeling of the spectra in implicit solvent improved the quantitative overlay of the carbonyl IR stretches, it led to an overall less significant assignment of absolute configuration.

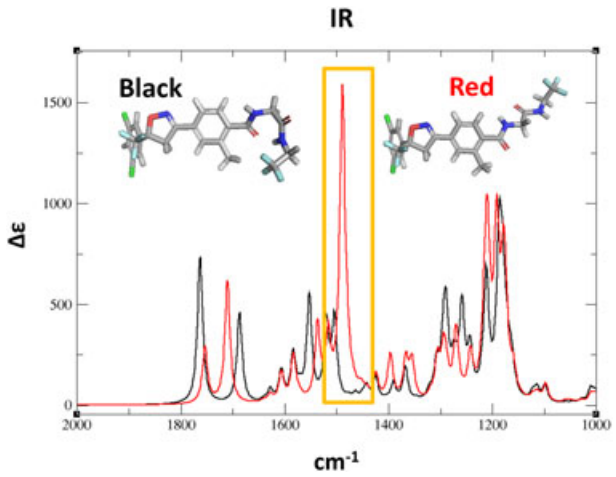

FIGURE 5 Overlay of calculated in vacuo IR showing effect of intramolecular hydrogen bonding (conformer 1 in black, conformer 5 in red). Large variation in computed IR observed in moving from an intramolecular hydrogen-bond-driven-folded conformation and the extended conformation. Orange box indicates the main peak associated with extended conformation amide NHs

3.6 | Explicit solvation of fluralaner

Attempts at quantitatively improving the overlay by modeling the conformational distribution and spectroscopy in implicit chloroform were extended to include modeling of explicit solvation using two molecules of $CHCl_3$. Since a hydrogen bond is most likely to form between the solvent and the carbonyl groups of fluralaner, we performed a conformational scan of a solvated complex beginning from the four dominant in vacuo conformations with added explicit solvent. The resultant conformational distribution is provided in Figure 7. Many complexes of relatively equivalent energy were identified, and it was clear that conformational sampling of the explicit complexes would be problematic since the available space was not exhaustively sampling. Additionally, sampling of solvated extended conformers was not pursued. Interestingly, the positions of the explicitly solvated carbonyls from the calculated IR were equivalent to the nonexplicit model of fluralaner in implicit solvent. This indicates that implicit solvation is successfully able to approximate the solvent shift effect on the carbonyls from a nonexplicitly solvated in vacuo model. Table 1 provides an overview of the match statistics for overlays shown in Figure 8 for the in vacuo explicit complex matching. The ESI for the electronic energy Boltzmann weighted spectra improves from 0.80 to 1.01, though the overall IR match is slightly worse.

3.7 | Explicit solvation of fluralaner in implicit chloroform

Short of modeling fluralaner in a chloroform solvent box, the best approximation of the physical environment from the experimental VCD determination is the first shell solvation (even if this is limited to only 2 solvent molecules in this case) in an implicit model of chloroform. From Table 1, it is clear that the same decrease in ESI is calculated when considering implicit solvent estimates for enantiomeric fit. From the overlay of the IR in Figure 9, it is apparent that the carbonyl peaks in the IR have shifted further to occupy positions at 1720 and 1650 cm^{-1}, positions which are now closely in-line with the experimental positions. This supports the notion that the in vacuo treatment of nonsolvated fluralaner can be used to fit the IR and VCD with the assumption that discrepancies in the position of the IR carbonyl peaks are artifacts due to the lack of proper solvation. Upon significant additional computational expense to model the solvation effects on the carbonyls, those peaks come into better alignment but offer no better statistical match when assigning absolute configuration. Owing to the same undersampling (since conformers are exactly those depicted in Figure 7) the VCD spectrum calculated with implicit treatment of the explicit complex also shows artifactual peaks in the carbonyl region.

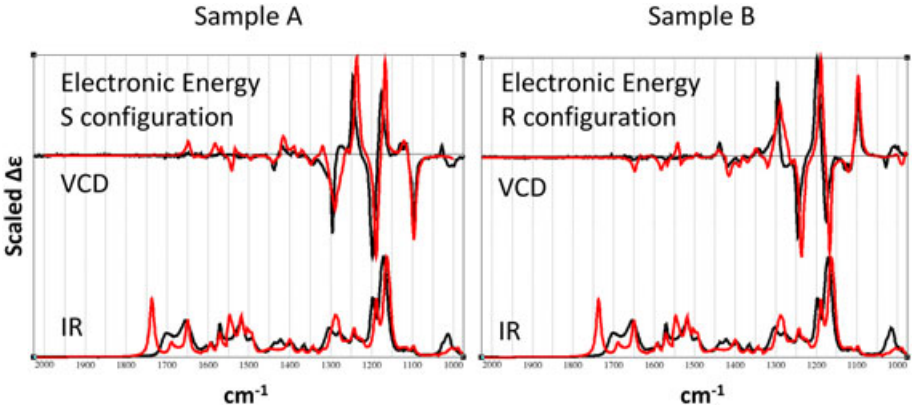

FIGURE 6 Overlay of implicit $CHCl_3$ IR and VCD spectra for Samples A and B (calculated spectra in red, experimental spectra in black)

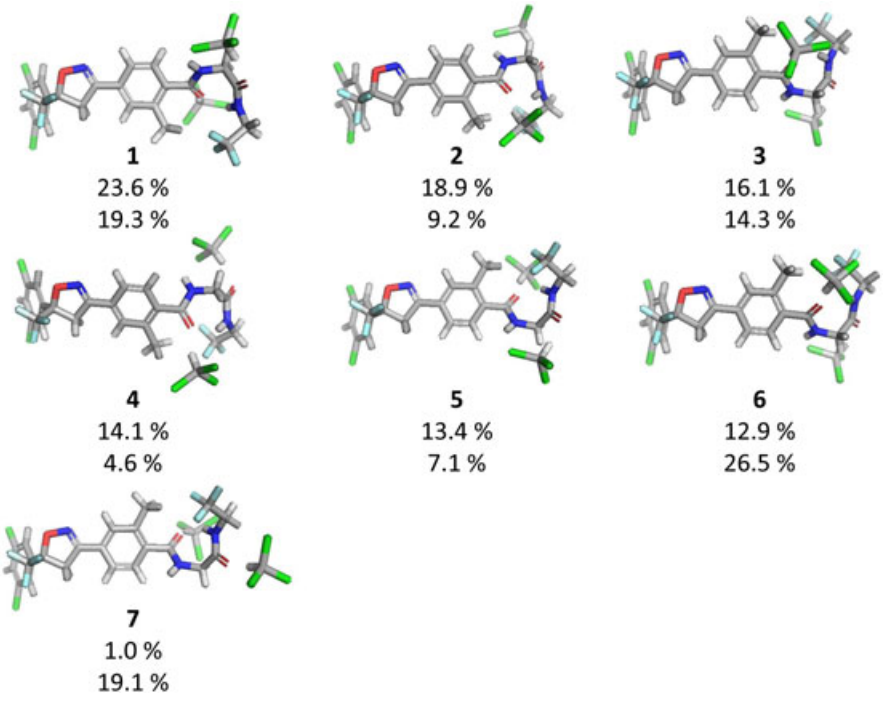

FIGURE 7 Conformations contributing to the Boltzmann distribution for explicitly solvated fluralaner using two molecules of $CHCl_3$. Electronic energy contribution (top) and free energy contribution (bottom) percentages are shown. Atom coloring: grey = carbon; red = oxygen; blue = nitrogen; green = chlorine; cyan = fluorine; white = hydrogen

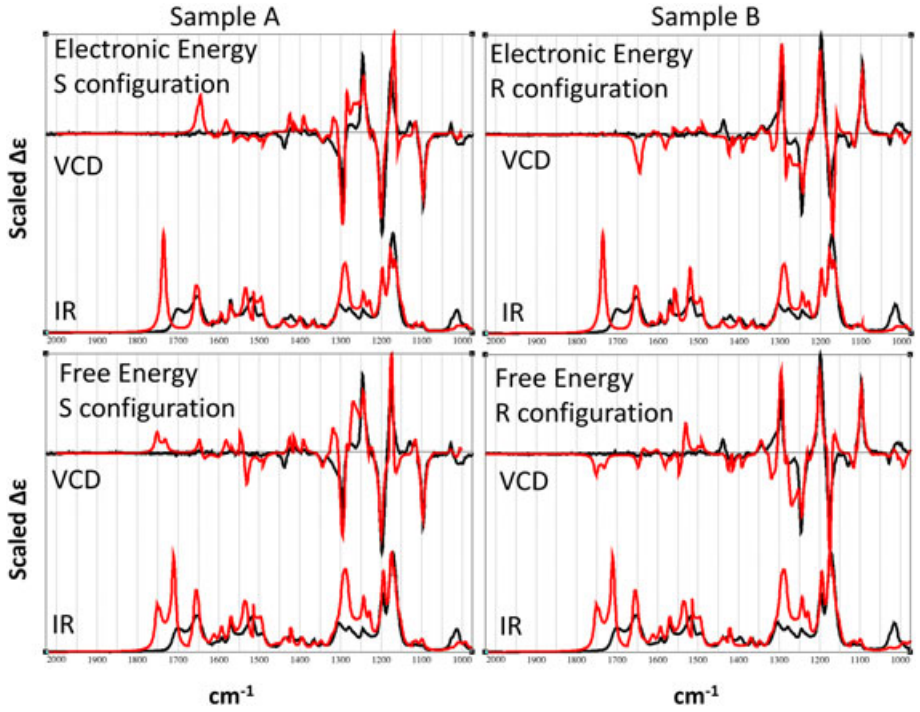

FIGURE 8 Overlay of explicit $CHCl_3$ IR and VCD spectra for Samples A and B (calculated spectra in red, experimental spectra in black)

3.8 | Assignment of absolute configuration using a fragment

A fragment-based approach can be pursued if the molecule of interest is significantly complex or flexible, or if computational resources are limited. Owing to advances in conformational sampling and computational resources, we have largely relied only on modeling complete structures.[5] A VCD and IR match will generally always be better when modeling the entire chemical species, and in turn, there will be more confidence in the assignment if approximations in structure are not made. However, we report our investigation of this approach since truncation of the amide tail led to a highly confident assignment of absolute configuration. Observations made here concerning the ability to truncate the assigned

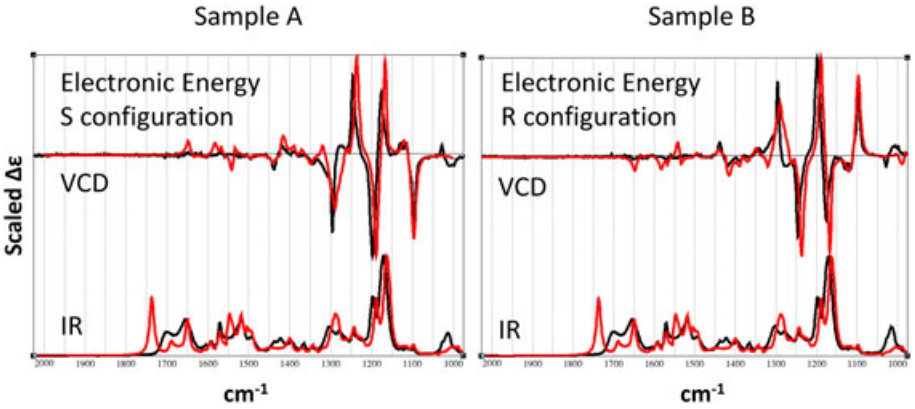

FIGURE 9 Overlay of explicit $CHCl_3$ in implicit $CHCl_3$ IR and VCD spectra for Samples A and B (calculated spectra in red, experimental spectra in black)

molecule and factors complicating assignment of flexible molecules have been made for some natural product linear diterpenes.[34]

The amide tail of fluralaner was truncated to provide the fragment compound displayed in Figure 10. There are only two in vacuo conformational minima for this species. This serves to greatly reduce the conformational search space, removes any ability for the formation of intramolecular hydrogen bonds, and deletes both carbonyls. As demonstrated earlier, the truncated carbonyls are not relevant due to their lack of presence in the experimental VCD spectrum. If the analysis of the full species is limited to the range of 1000 to 1500 cm^{-1}, the match remains consistent (Figure S1 and Table 1).

Figure 11 provides the overlays of the IR and VCD for the (*S*)-enantiomer of the fragment onto the experimental spectra of Sample A over the full and truncated spectral ranges. While the VCD and IR match are very good over most of the range, it is clear that matching the fragment fails to include IR content of the amides so the match in this region is quite poor. Statistics of the fragment match provided in Table 1 indicate that the correct absolute configuration for Samples A and B could have been made with IR overlap of 0.61 to 0.74 and ESI of approximately 0.90. In this case, completely ignoring the carbonyls in the calculated structure still provides enough chemical information in the IR and VCD to properly assign absolute configuration.

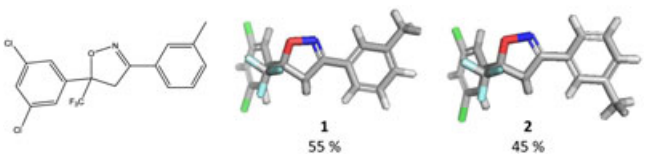

FIGURE 10 Conformations contributing to the Boltzmann conformational distribution of the (*R*) configuration of the fragment. Electronic energy contribution percentages are shown. Atom coloring: grey = carbon; red = oxygen; blue = nitrogen; green = chlorine; cyan = fluorine; white = hydrogen

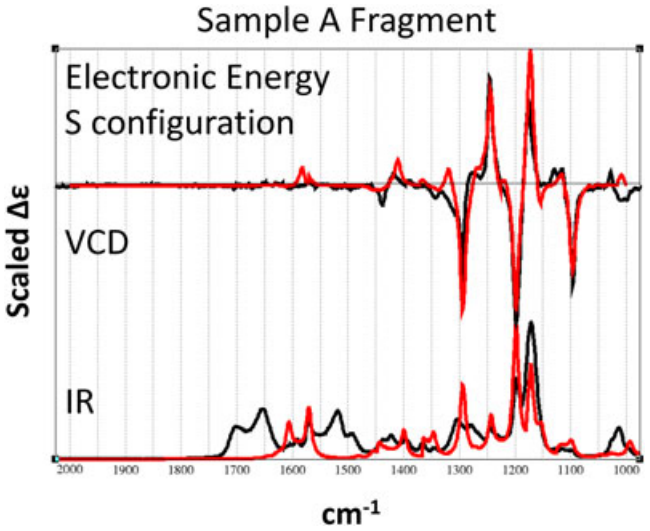

FIGURE 11 Overlay of in vacuo IR and VCD spectra for Sample A onto the fragment (calculated spectra in red, experimental spectra of fluralaner in black)

4 | CONCLUSION

Absolute configuration assignment of fluralaner using VCD indicated that the active (+)-enantiomer of the racemic mixture has the (*S*) configuration. This assignment supports the previous crystallographic determination that the active enantiomer or (+)-fluralaner is (*S*). The absence of carbonyl peaks in the experimental VCD was shown, through a set of computational studies, to be caused by averaging of the conformationally dependent positive and negative peaks in the VCD spectrum. Reducing the range of the match to ignore the carbonyls or truncating the chemical structure provided equivalent matching

and proper assignment of the (*S*) configuration. When VCD and IR spectra are compared and all functional groups are not apparent in both spectra, it can be indicative of conformational averaging of some structural features. When conformational ensembles provide a calculated Boltzmann weighted spectrum which contains peaks in the regions with no experimental peak intensity, it may be a sign of undersampling in the conformational search. While calculation of spectra using implicit and explicit solvation would be expected to better approximate the spectroscopic environment, it was determined that a confident assignment of absolute configuration could be made using only in vacuo calculations.

ACKNOWLEDGMENTS

We thank the MRL modeling tools development group, especially Joe Shpungin for work on implementing a conformational sampling routine.

ORCID

Leo A. Joyce http://orcid.org/0000-0002-8649-4894
Edward C. Sherer http://orcid.org/0000-0001-8178-9186

REFERENCES

1. McConathy J, Owens MJ. Stereochemistry in drug action. *Prim Care Companion J Clin Psychiatry*. 2003;5:70-73.
2. Chhabra N, Aseri ML, Padmanabhan D. A review of drug isomerism and its significance. *Int J Appl Basic Med Res*. 2013;3:16-18.
3. Ozoe Y, Asahi M, Ozoe F, Nakahira K, Mita T. The antiparasitic isoxazoline A1443 is a potent blocker of insect ligand-gated chloride channels. *Biochem Biophys Res Commun*. 2010;391:744-749.
4. He J, Polavarapu PL. Determination of intermolecular hydrogen bonded conformers of alpha-aryloxypropanoic acids using density functional theory predictions of vibrational absorption and vibrational circular dichroism spectra. *J Chem Theory Comput*. 2005;1:506-514.
5. Sherer EC, Lee CH, Shpungin J, et al. Systematic approach to conformational sampling for assigning absolute configuration using vibrational circular dichroism. *J Med Chem*. 2014;57:477-494.
6. Stephens PJ, McCann DM, Devlin FJ, Smith AB 3rd. Determination of the absolute configurations of natural products via density functional theory calculations of optical rotation, electronic circular dichroism, and vibrational circular dichroism: the cytotoxic sesquiterpene natural products quadrone, suberosenone, suberosanone, and suberosenol a acetate. *J Nat Prod*. 2006;69:1055-1064.
7. Debie E, De Gussem E, Dukor RK, Herrebout W, Nafie LA, Bultinck P. A confidence level algorithm for the determination of absolute configuration using vibrational circular dichroism or Raman optical activity. *Chemphyschem*. 2011;12:1542-1549.
8. Freedman TB, Cao XL, Dukor RK, Nafie LA. Absolute configuration determination of chiral molecules in the solution state using vibrational circular dichroism. *Chirality*. 2003;15:743-758.
9. Batista JM, Bolzani VS. Determination of the Absolute Configuration of Natural Product Molecules Using Vibrational Circular Dichroism. In: Atta-ur-Rahman, ed. *Studies in Natural Products Chemistry*. Oxford: Elsevier; 2014;41:383-417.
10. Burgueno-Tapia E, Joseph-Nathan P. Vibrational circular dichroism: recent advances for the assignment of the absolute configuration of natural products. *Nat Prod Commun*. 2015;10:1785-1795.
11. Burgueño-Tapia E, Joseph-Nathan P. Vibrational circular dichroism: recent advances for the assignment of the absolute configuration of natural products. *Nat Prod Commun*. 2017;12:641-651.
12. Joseph-Nathan P, Gordillo-Roman B. Vibrational circular dichroism absolute configuration determination of natural products. In: Kinghorn AD, Falk H, Gibbons S, Kobayashi J, eds. *Progress in the chemistry of organic natural products*. New York: Springer; 2015;100:311-452.
13. Butora G, Qi N, Fu W, Nguyen T, Huang HC, Davies IW. Cyclic-disulfide-based prodrugs for cytosol-specific drug delivery. *Angew Chem Int Ed*. 2014;53:14046-14050.
14. Li H, Chen CY, Nguyen H, et al. Asymmetric synthesis of cyclic indole aminals via 1,3-stereoinduction. *The J Org Chem*. 2014;79:8533-8540.
15. Liu Z, Shultz CS, Sherwood C, et al. Highly enantioselective synthesis of anti aryl beta-hydroxy alpha-amino esters via dkr transfer hydrogenation. *Tet Lett*. 2011;52:1685-1688.
16. Pero JE, Rossi MA, Kelly MJ 3rd, et al. Optimization of novel aza-benzimidazolone mGluR2 PAMs with respect to LLE and PK properties and mitigation of CYP TDI. *ACS Med Chem Lett*. 2016;7:312-317.
17. Sauri J, Bermel W, Buevich AV, et al. Homodecoupled 1,1- and 1,n-ADEQUATE: pivotal NMR experiments for the structure revision of Cryptospirolepine. *Angew Chem Int Ed*. 2015;54:10160-10164.
18. Singh SB, Kaelin DE, Wu J, et al. Tricyclic 1,5-naphthyridinone oxabicyclooctane-linked novel bacterial topoisomerase inhibitors as broad-spectrum antibacterial agents-SAR of left-hand-side moiety (Part-2). *Bioorg Med Chem Lett*. 2015;25:1831-1835.
19. Becke AD. Density-functional thermochemistry. III. The role of exact exchange. *J Chem Phys*. 1993;98:5648-5652.
20. Francl MM, Pietro WJ, Hehre WJ, et al. Self-consistent molecular-orbital methods .23. A polarization-type basis set for 2nd-row elements. *J Chem Phys*. 1982;77:3654-3665.
21. Hehre WJ, Ditchfield R, Pople JA. Self-consistent molecular orbital methods. 12. Further extensions of Gaussian-type basis sets for use in molecular-orbital studies of organic-molecules. *J Chem Phys*. 1972;56:2257-2261.
22. Lee CT, Yang WT, Parr RG. Development of the Colle-Salvetti correlation-energy formula into a functional of the electron-density. *Phys Rev B*. 1988;37:785-789.

23. Miehlich B, Savin A, Stoll H, Preuss H. Results obtained with the correlation-energy density functionals of Becke and Lee, Yang and Parr. *Chem Phys Lett*. 1989;157:200-206.

24. Petersson GA, Allaham MA. A complete basis set model chemistry .2. Open-shell systems and the total energies of the 1st-row atoms. *J Chem Phys*. 1991;94:6081-6090.

25. Petersson GA, Bennett A, Tensfeldt TG, Allaham MA, Shirley WA, Mantzaris J. A complete basis set model chemistry .1. The Total energies of closed-Shell atoms and hydrides of the 1st-row elements. *J Chem Phys*. 1988;89:2193-2218.

26. Rassolov VA, Pople JA, Ratner MA, Windus TL. 6-31G* basis set for atoms K through Zn. *J Chem Phys*. 1998;109:1223-1219.

27. Rassolov VA, Ratner MA, Pople JA, Redfern PC, Curtiss LA. 6-31G*basis set for third-row atoms. *J Comput Chem*. 2001;22:976-984.

28. Marenich AV, Cramer CJ, Truhlar DG. Universal solvation model based on solute electron density and on a continuum model of the solvent defined by the bulk dielectric constant and atomic surface tensions. *J Phys Chem B*. 2009;113:6378-6396.

29. Frisch MJ, Trucks GW, Schlegel HB, et al. *Gaussian 09, Revision D.01*. Wallingford, CT: Gaussian, Inc.; 2009.

30. Cheeseman JR, Frisch MJ, Devlin FJ, Stephens PJ. Ab initio calculation of atomic axial tensors and vibrational rotational strengths using density functional theory. *Chem Phys Lett*. 1996;252:211-220.

31. Shen J, Zhu C, Reiling S, Vaz R. A novel computational method for comparing vibrational circular dichroism spectra. *Spectrochimica acta*. 2010;76:418-422.

32. Nicu VP, Baerends EJ. Robust normal modes in vibrational circular dichroism spectra. *Phys Chem Chem Phys*. 2009;11:6107-6118.

33. Nicu VP, Debie E, Herrebout W, Van der Veken B, Bultinck P, Baerends EJ. A VCD robust mode analysis of induced chirality: the case of pulegone in chloroform. *Chirality*. 2009;21(Suppl 1): E287-E297.

34. Merten C, Smyrniotopoulos V, Tasdemir D. Assignment of absolute configurations of highly flexible linear diterpenes from the brown alga Bifurcaria Bifurcata by VCD spectroscopy. *Chem Commun*. 2015;51:16217-16220.

SUPPORTING INFORMATION

Additional Supporting Information may be found online in the supporting information tab for this article.

How to cite this article: Kong J, Joyce LA, Liu J, Jarrell TM, Culberson JC, Sherer EC. Absolute configuration assignment of (+)-fluralaner using vibrational circular dichroism. *Chirality*. 2017;1–11. https://doi.org/10.1002/chir.22770